Plasmonics (2023) 18:727–734
https://doi.org/10.1007/s11468-023-01798-w

Effect of Uniform Strain on Graphene Surface Plasmon Excitations

C. Lemus[1] · **G. Gonzalez de la Cruz**[1] · **M. Oliva-Leyva**[2]

Received: 24 December 2022 / Accepted: 3 February 2023 / Published online: 21 February 2023

Abstract
This paper reports a study of the reflectance of the optical sensors based on graphene under uniform strain. Assuming the graphene layer is surrounded by two different semi-infinite dielectric media, the generalized Fresnel coefficients are derived as a function of usual quantities (e.g., dielectric constants, incident angles, and strain) and anisotropic optical conductivity. The strain not only changes the electronic band structure but also can be employed to tune the electronic collective excitations (plasmons) and thus the optical reflectance of graphene monolayers. One of the most common techniques for plasmon excitation is the Kretschmann configuration. It is based on the observation of a sharp minimum in the reflection coefficient versus the angle (or wavelength) curve. Because strain induces anisotropy in graphene optical conductivity the strain-dependent orientation plays an important role to manipulate the variation of graphene plasmon energy, which may be useful to synchronize graphene properties in plasmonic devices to enhance light-matter interactions.

Keywords Graphene · Strain · Plasmons · Reflectance

Introduction

Surface plasmons (SPs) are transverse magnetic (TM) polarized electromagnetic waves coupled with charge density oscillations (plasmons) traveling along the metal–dielectric interface. The electric field associated with these oscillations decay exponentially into the dielectric medium making plasmons extremely sensitive to the refractive index of the medium. When the wave vector of the incident light matches the wave vector of the SP wave, the SP resonantly couples with the incident light, and a remarkable electric field enhancement can be realized, and the so-called SP resonance occurs. Usually, surface plasmons can be excited via evanescent waves in the Kretchmann configuration utilizing high-index prisms where the wavevector mismatch between vacuum and SP is compensated [1]. Once the SP is excited in the Kretchmann configuration, partially of the energy associated to the incident electromagnetic radiation will be transferred to the SP, and a sharp minimum is observed in the reflectance versus angle (or wavelength) curve. The ability of controlling strong light-matter interaction through surface plasmons in metals has driven the field of plasmonics. Additionally, increasing research has been carried out to investigate and manipulate SP for new sensing functionalities. Based on this principle, different architectures of plasmonic sensors involving metals have been designed in previous years [2, 3]. However, the major obstacle in developing plasmonic applications in metallic devices is dissipative loss, which limits the propagation length of surface plasmons and broadens the bandwidth of surface plasmon resonances and their surfaces easily oxidize degrading their plasmonic characteristics [4]. To overwhelm these deficiencies, some new structures have been proposed to investigate surface plasmon resonances for new plasmonic materials; among them, graphene has emerged as an alternative, unique two- dimensional material able to extend the field of plasmonics for terahertz to mid-infrared applications [5–7]. Graphene is a two-dimensional material made of carbon atoms arranged in hexagonal lattice, graphene material has attracted tremendous attention due to electrical, optical, and chemical properties which can be tunable to external parameters, including voltage-induced doping, selective substrate interactions, or strain engineering. Two-dimensional plasmons in graphene exhibit unique optoelectronic properties and mediate extraordinary light–matter interactions. Therefore, these exceptional properties make graphene a

✉ G. Gonzalez de la Cruz
bato@fis.cinvestav.mx

[1] Departamento de Física, CINVESTAV-IPN, Apartado Postal 14-740, CDMX, Mexico

[2] Departamento de Física, Facultad de Ciencias, UNAM, 04510 CDMX, Mexico

promising candidate for innovative plasmonic devices and possible applications in photonics, optoelectronics, and in sensor technologies [8]. Due to the fundamental mismatch between the surface plasmon supported by a graphene monolayer and that of wave vector of light, such coupling is basically weak and plasmonic crystals are required to enhance it to achieve adequate efficiency for practical device applications. Concerning this purpose, artificially engineering structures (or metamaterials) have been used as a platform for improving light-mater interaction in the last years. Hence, in the context of potential applications the exploration of graphene plasmons with metamaterials plays an important task in plasmonics and, studying the interactions of the plasmon modes in multilayer graphene structures with metallic or dielectric substrates offer new opportunities for applications and fundamental studies of collective electron excitations in plasmonic metamaterials for biological and chemical sensing [9–17], photodetectors [18] and optoelectronics [19, 20]. Additionally, plasmon properties in double-layer graphene and multilayer graphene systems considering the effects of temperature, spin-polarized in the presence of the external magnetic field, and applied electric field have been reported [21–25].

When a graphene layer is subjected to mechanical strain, it does not break the lattice symmetry but somewhat the high-symmetrical points of the Brillouin zone are modified in such a way the Dirac cones located in graphene at points K and K´ move in opposite directions [26, 27]. It has been shown that monolayer graphene can tolerate stretching deformations as large as 20% without substantially destroying its crystal structure but opens a gap above this threshold.

This large elastic deformation affects substantially the graphene energy band structure and therefore, it is thermal, optical properties and other plasmonic properties [28–30]. On the other hand, the influence of the strain on several electronic properties produces also a significantly changes on the electronic polarizability and thereby collective electronic excitations associated with anisotropic honeycomb lattice [31–33].

In this work, we theoretically investigate plasmon dispersion and optical reflectance of mono graphene structures under uniform strain. For this purpose, we make use of the linear response theory and the Kubo formalism to calculate the induced charge density, related with the anisotropic optical conductivity through the charge conservation equation. We have found analytical and numerical results displaying the effect of strain on the electronic charge density excitations in the long-wave limit by varying several parameters, as the angle given the direction of the applied strain, the separation of the layers, etc. It is worth noting that collective charge density excitations and optical reflectance can efficiently controlled by strain, and it is possible to overcome the mismatch between the momentum of the surface plasmon and that of incident radiation and thereby improve the light-matter interaction. Usually, surface plasmon can be excited via evanescent waves using the Kretschmann configuration, Once, surface plasmon is excited in the Kretschmann configuration, a sharp minimum is observed in the reflection coefficient versus incident angle (or wavelength) curve. Recently [34], a theoretical study of the dispersion of linearly polarized light between two dielectric media separated by an anisotropic graphene under oblique incidence has been reported considering the unstrained high-frequency optical conductivity (equal to $e^2/4\hbar$ for $\hbar\omega > 2E_f$ where E_f is the Fermi energy), the optical response of graphene is limited by the fine-structure constant $\alpha \approx 1/137$, which describes the coupling between light and relativistic electrons in quantum electrodynamics.

Additionally, plasmons at low frequencies in anisotropic Dirac systems have been theoretically studied [35], these authors showed that the strong anisotropy can be used to guide the plasmon modes with new properties in the field of plasmonics. Also, plasmons modes in one and double-layer black phosphorous structures under uniaxial strain have been reported [36], they found that the strain-dependent orientation can be considered to control the variations of the plasmon energy.

Theoretically Model

In-plane graphene sheet under uniform strain appreciably modify its electronic band structure around the Fermi level, which induces anisotropy in the hoping parameters in the tight-band model. Our studied system, selecting the Cartesian system in the x-axis along the graphene zigzag direction of the lattice, the strain tensor reads

$$\vec{\varepsilon} = \varepsilon \begin{pmatrix} cos^2\theta - \rho sin^2\theta & (1+\rho)cos\theta sin\theta \\ (1+\rho)cos\theta sin\theta & sin^2\theta - \rho cos^2\theta \end{pmatrix} \quad (1)$$

where ε is the strain modulus, θ denotes the angle between the applied tension and the x-axis, and ρ being the Poisson ratio. The shift of the Dirac cones under uniaxial strain can be explained and quantitatively described by a combination of a tight-binding approximation and linear elasticity theory [37]. The frequency-dependent conductivity tensor of graphene under uniform strain can be written as [38]

$$\overleftrightarrow{\sigma(\omega)} = \sigma(\omega)[I + 2\Delta - Tr(\Delta)] \quad (2)$$

where $\boldsymbol{\Delta} = -\boldsymbol{\beta}\,\vec{\varepsilon}$, $\boldsymbol{\beta} \sim \mathbf{1.1}$ is the electron Gruneisen parameter, and $\sigma(\omega)$ is the optical conductivity which considers the contribution of the intraband and interband electronic transitions in unstrained graphene,

$$\sigma_{\text{intra}} = \frac{2ie^2 k_B T}{\pi(\omega + i\Gamma)} ln\left[2cosh\left(\frac{E_f}{2k_B T}\right)\right] \quad (3)$$

and

$$\sigma_{inter} = \frac{e^2}{4}\left[\frac{1}{2} + \frac{1}{\pi} + arctan\left(\frac{\omega - E_f}{2k_{BT}}\right) - \frac{i}{2\pi}\ln\frac{\left(\omega + E_f\right)^2}{\left(\omega - E_f\right)^2 + (2k_BT)^2}\right] \tag{4}$$

Within the linear-response theory, plasmon modes can be described as the zeros of the dielectric function $\varepsilon(q,\omega)$, which depends on the density–density correlation function, i.e., the polarization of the non-interacting electron gas $\varepsilon(q,\omega) = 1 - V_q\Pi(q,\omega)$ and $V_q = 2\pi e^2/\varepsilon_0 q$ is the Fourier transform of the two-dimensional Coulomb electron–electron interaction and ε_0 the dielectric constant of the medium. Because we are interested in the linear-response function to smoothly varying external potential $\varphi_{ext}(q,\omega)$, the charge density induced in the two-dimensional electron gas in graphene up first order approximation in $\varphi_{ext}(q,\omega)$ is $\rho_{ind}(q,\omega) = e^2\Pi(q,\omega)\varphi_{ext}(q,\omega)$ and satisfies the usual continuity equation of electrodynamics [39]

$$i\omega\Pi(q,\omega) - q_\mu\sigma_{\mu\nu}(\omega)q_\nu = 0 \tag{5}$$

Finally, from Eqs. (8)–(10) and at low energy approximation such that $\omega << 2E_f$ the interband part Eq. (10) is negligible comparing to the intraband part. Therefore, in the low energy approximation range, the optical conductivity is well described by the Drude-like surface conductivity. For $E_f >> k_BT$ the optical conductivity depends linearly on the Fermi energy

$$\sigma_g(\omega) = \frac{e^2E_f}{\pi}\frac{i}{\omega + i\Gamma}\left(1 - \frac{\omega^2}{4E_f^2}\right) \tag{6}$$

where $\boldsymbol{q} = q(cos\varphi,\ sin\varphi)$ is the wave vector associated with the charge fluctuations induced in the strained graphene. Thus, it follows that the electron polarizability for graphene under uniaxial strain results in ($\omega >> \Gamma$)

$$\Pi(q,\omega) = \frac{E_f}{\pi}\frac{q^2}{\omega^2}\left(1 - \frac{\omega^2}{4E_f^2}\right)[1 - 2\beta(1+\rho)\varepsilon\ \cos(2\theta - 2\varphi)] \tag{7}$$

As can be observed, in linear response theory, the deformed graphene presents an anisotropic optical response given by Eq. (2) and as a consequence, the non-interacting graphene electron polarizability depends on the strain modulus and the direction of the applied uniform strain. It is worth to noting that in the absence of strain, i.e., $\varepsilon = 0$, the graphene electron polarizability at long wavelength approximation is recovered [40]. One thus finds, that at low frequencies with the graphene electron polarizability, Eq. (7), and equaling the dielectric function $\varepsilon(q,\omega) = 1 - V_q\,\Pi(q,\omega)$ to zero, we arrive at the following equation for the surface plasmon of graphene under uniform strain

$$\omega^2(q) = \frac{4e^2E_f}{\varepsilon_1 + \varepsilon_2}q[1 - 2\beta(1+\rho)\varepsilon\cos(2\theta - 2\varphi)] \tag{8}$$

It can be seen the plasmon energy remains the dependence of $q^{1/2}$ which is a characteristic of the two-dimension electron gas system, and it is maximum when it propagates perpendicular to the applied strain and minimum for $\theta = \varphi$. These latter properties of the graphene plasmon modes allow us to manipulate the plasmon energy and enhance light-matter interactions in plasmonic metamaterials. In Fig. 2a, the optical plasmon modes are depicted as a function of the wave vector for different values of the stretching in the amchair direction ($\theta - \varphi = 0$), as it is shown the plasmon energy decreases for large values of the applied strain in this particular direction. On the other hand, the dependence of optical plasmons as a function of the plasmon wave vector is shown in Fig. 2b for different directions of the applied strain. As can be observed, the optical plasmon energy is free landau damping in the long wave limit and it increase with increasing values of the direction of the applied stretching and reach its maximum value when the plasmon wave vector and the applied strain are orthogonal to each other (θ-$\varphi = \pi/2$). However, as q increases, it is expected that the plasmon dispersion relation of the graphene layer under strain decay into the continuum of the interband single particle excitation region.

Generalized Fresnel Equations

To investigate the reflection of a linearly polarized electromagnetic wave through two semi-infinite dielectric media with dielectric constants ε_1 and ε_2 separated by a deformed graphene layer located at $z = 0$, whose optical conductivity is characterized by the second-order symmetric tensor given by Eq. (2). As depicted in Fig. 1, if the x–y plane is the interface plane, for wave propagation in the x direction, the magnetic field for p polarization, the magnetic field is polarized along the y-direction and can be written in the form $\boldsymbol{H} = (0,\ Ae^{iqz} + Be^{-iqz},\ 0)e^{i\kappa x - i\omega t} = (0,\ \Phi_p,\ 0)$ and the electric field associated with this electromagnetic wave is $\boldsymbol{E} = -c/i\omega\varepsilon_s(-\partial_z\Phi_p,\ 0,\ \partial_x\Phi_p)$ with $q_s = (\varepsilon_s\,\omega^2/c^2\text{-}\kappa^2)^{1/2}$ ($s = 1,2$) and c the light velocity in vacuum. Furthermore, for s polarization the electric filed is polarized along the y-direction, i.e., $\boldsymbol{E} = (0,\ Ce^{iqz} + De^{-iqz},\ 0)e^{i\kappa x - i\omega t} = (0,\ \Phi_s,\ 0)$ and $\boldsymbol{H} = c/i\omega\mu(-\partial_z\Phi_s,\ 0,\ \partial_x\Phi_s)$ with $\mu = 1$, the magnetic permittivity.

The electric and magnetic fields at the interface can be related by the following boundary conditions

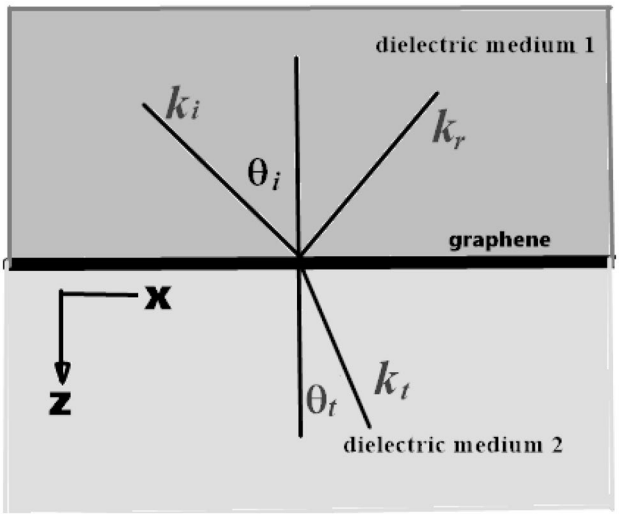

Fig. 1 Schematic representation of the scattering geometry for oblique incidence with incident angle $\boldsymbol{\theta_i}$ between two different dielectric media with strained graphene separating them

$$\boldsymbol{n\ x\ (E_2 - E_1)_{z=0} = 0}$$

$$\boldsymbol{n\ x\ (H_2 - H_1)_{z=0} = J} \tag{9}$$

where $\boldsymbol{n}$ is the unit vector normal to the surface and $\boldsymbol{J}$ is the surface current density of the graphene under uniform strain, and is given by $\boldsymbol{J = \sigma E}$, namely

$$J_x = \sigma_{xx}E_x + \sigma_{xy}E_y, \quad J_y = \sigma_{yx}E_x + \sigma_{yy}E_y \tag{10}$$

with σ_{ij} being the components of the graphene tensor conductivity. Applying the boundary condition from Eq. (9), the field coefficients in the medium 1 can be related with the field coefficients of the medium 2 as follows [34, 41, 42],

$$\begin{pmatrix} A_1 \\ B_1 \\ C_1 \\ D_1 \end{pmatrix} = D \begin{pmatrix} A_2 \\ B_2 \\ C_2 \\ D_2 \end{pmatrix} \tag{11}$$

Here, D represents the transfer matrix connecting the coefficients at adjacent monolayer graphene and it is given by

$$D = \frac{1}{2}\begin{pmatrix} \left(\frac{q_2}{\varepsilon_2}\left(\frac{\varepsilon_1}{q_1} + \frac{\varepsilon_2}{q_2} + \frac{4\pi}{\omega}\sigma_{xx}\right)\right. & \frac{q_2}{\varepsilon_2}\left(-\frac{\varepsilon_1}{q_1} + \frac{\varepsilon_2}{q_2} - \frac{4\pi}{\omega}\sigma_{xx}\right) & \frac{4\pi}{\omega}\sigma_{xy} & \frac{4\pi}{\omega}\sigma_{yx} \\ \left(\frac{q_2}{\varepsilon_2}\left(-\frac{\varepsilon_1}{q_1} + \frac{\varepsilon_2}{q_2} + \frac{4\pi}{\omega}\sigma_{xx}\right)\right. & \frac{q_2}{\varepsilon_2}\left(\frac{\varepsilon_1}{q_1} + \frac{\varepsilon_2}{q_2} - \frac{4\pi}{\omega}\sigma_{xx}\right) & \frac{4\pi}{\omega}\sigma_{xy} & \frac{4\pi}{\omega}\sigma_{yx} \\ \frac{4\pi}{cq_1}\frac{q_2}{\varepsilon_2}\sigma_{xy} & -\frac{4\pi}{cq_1}\frac{q_2}{\varepsilon_2}\sigma_{xy} & \frac{\omega}{cq_1}\left(\frac{cq_1}{\omega} + \frac{cq_2}{\omega} + \frac{4\pi}{\omega}\sigma_{yy}\right) & \frac{\omega}{cq_1}\left(\frac{cq_1}{\omega} - \frac{cq_2}{\omega} + \frac{4\pi}{\omega}\sigma_{yy}\right) \\ \frac{-4\pi}{cq_1}\frac{q_2}{\varepsilon_2}\sigma_{xy} & \frac{4\pi}{cq_1}\frac{q_2}{\varepsilon_2}\sigma_{xy} & \frac{\omega}{cq_1}\left(\frac{cq_1}{\omega} - \frac{cq_2}{\omega} - \frac{4\pi}{\omega}\sigma_{yy}\right) & \frac{\omega}{cq_1}\left(\frac{cq_1}{\omega} + \frac{cq_2}{\omega} - \frac{4\pi}{\omega}\sigma_{yy}\right) \end{pmatrix} \tag{12}$$

As can be observed from these equations, in general, in the reflected waves the polarization of the incident wave is not conserved due to the anisotropy of the tensor conductivity associated to the graphene under uniform strain. In addition, the transmitted waves also include both s and p polarization waves. Namely, the incident s or p light polarization is only preserved if $\sigma_{xy} = 0$. With the transfer matrix, we can easily calculate the optical spectra such as reflection, transmission, and absorption for the deformed graphene. Assuming that the incident light is p-polarized, Eq. (11) reduces to [42]

$$\begin{pmatrix} A_1 \\ B_1 \\ 0 \\ D_1 \end{pmatrix} = D \begin{pmatrix} A_2 \\ 0 \\ C_2 \\ 0 \end{pmatrix} \tag{13}$$

in terms of the elements of the transfer matrix D, the reflection and transmission coefficients can be written as

$$R = \left|\frac{D_{23}D_{23} - D_{33}D_{21}}{D_{13}D_{32} - D_{11}D_{33}}\right|^2 + \frac{\varepsilon_1}{c^2}\left[\frac{D_{43}D_{31} - D_{41}D_{33}}{D_{13}D_{32} - D_{11}D_{33}}\right]^2,$$

$$T = \left[\frac{D_{33}}{D_{13}D_{32} - D_{11}D_{33}}\right]^2 + \frac{\varepsilon_1}{c^2}\left|\frac{D_{31}}{D_{13}D_{31} - D_{11}D_{33}}\right|^2 \tag{14}$$

where the first and second terms on the right size of Eq. (14) represent the contribution of the reflectance and transmission of p and s waves, respectively. It is worth mention that when the strain vanishes ($\varepsilon = 0$) thus $\sigma_{xy} = 0$, and the reflection and transmission coefficient for a single graphene layer embedded in dielectric constants ε_1 and ε_2 are like that obtained in Ref. [43].

Numerical Results

As we mentioned before, the zeros of the dielectric constant of monolayer graphene under uniform strain give the relation dispersion of the plasmon modes given by Eq. (8) which in general, will depend on the graphene parameters and the applied strain. Graphene plasmon excitations exist and are free landau damping into the intraband and interband single

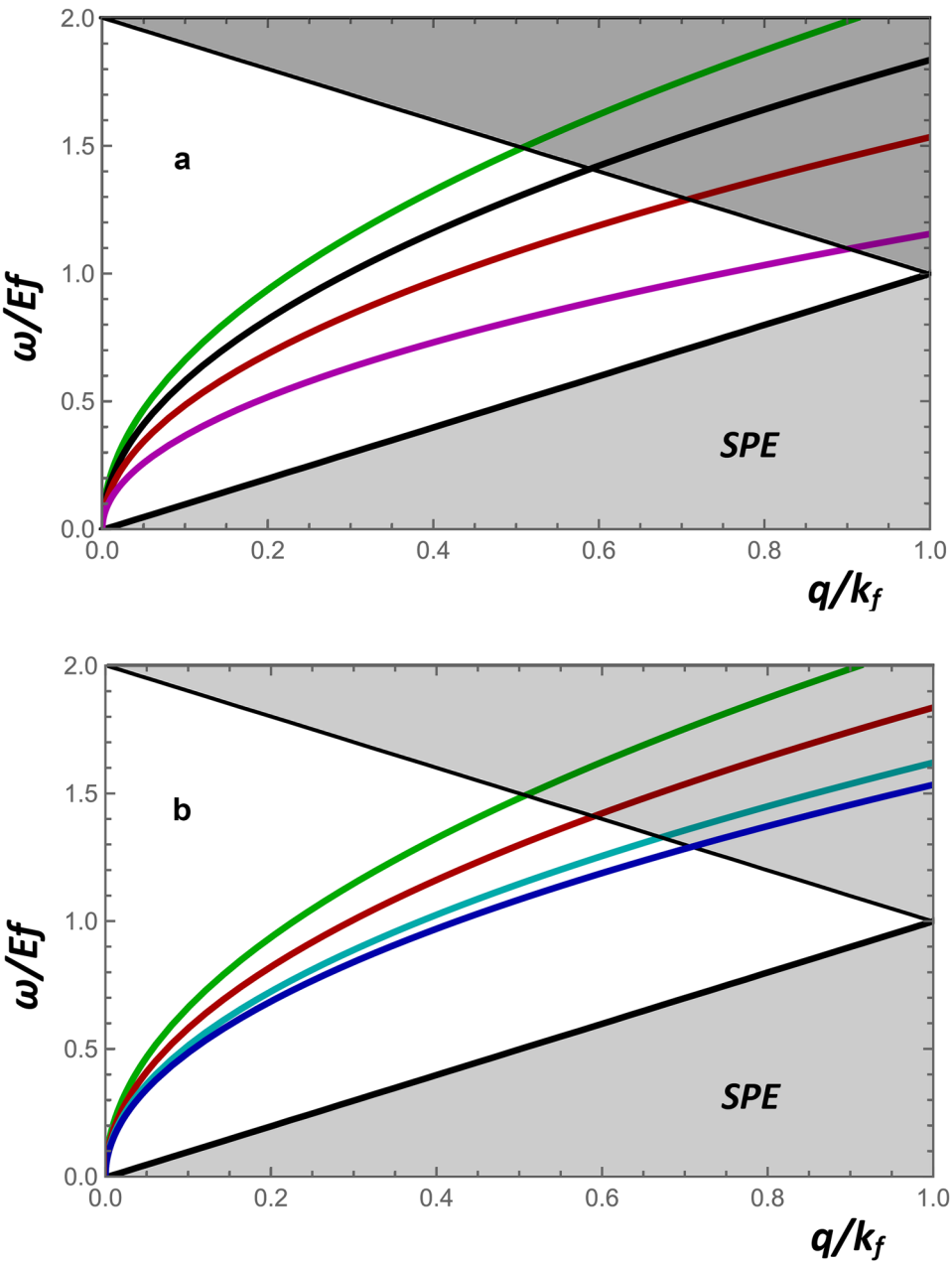

Fig. 2 **a** Plasmon dispersion relation for graphene for different applied uniform strain along the plasmon wave propagation, i.e., $\theta - \varphi = 0$, $\varepsilon_1 = \varepsilon_2 = 1$ and Fermi energy $E_f = 0.5\ eV$. $\varepsilon = 0.0$ (Green), $\varepsilon = 0.05$ (Black), $\varepsilon = 0.1$ (Red), $\varepsilon = 0.15$ (Purple). **b** Similar to panel (**a**) but for different directions of the uniaxial strain of magnitude $\varepsilon = 0.1$. $\theta - \varphi = 0$ (Blue), $\theta - \varphi = \pi/6$ (Cyan), $\theta - \varphi = \pi/3$ (Red), $\theta - \varphi = \pi/2$ (Green)

particle excitations where $\omega > \gamma q$ and $2E_f - \gamma q > \omega$ and the electron polarizability $\Pi(q, \omega)$ is real In Fig. 2a, the optical plasmon modes are depicted as a function of the wave vector for different values of the stretching in the direction such that $\theta - \varphi = 0$, as it is shown the plasmon energy decreases for large values of the applied strain along the plasmon propagation. On the other hand, the dependence of optical plasmons as function of the plasmon wave vector for fixed applied strain is shown in Fig. 2b for different directions of the applied strain. As can be observed, the optical plasmon energy is free landau damping in the long wave limit and it increase with increasing the direction of the applied stretching and reach its maximum value when the plasmon wave vector and the applied strain are orthogonal to each other ($\theta - \varphi = \pi/2$). However, as q increases, it is expected that the plasmon dispersion relation of the graphene layer under strain decay into the continuum of the interband single particle excitation region. Because strain induces anisotropy in graphene optical conductivity, the strain-dependent orientation plays an important role to manipulate the variations of the graphene plasmon energy, which may be useful to tune graphene properties in plasmonic devices to manipulate light-matter interaction.

Usually, surface plasmon can be excited via evanescent waves in the Kretschmann configuration, utilizing high-index prisms, where the wave vector matching between incident

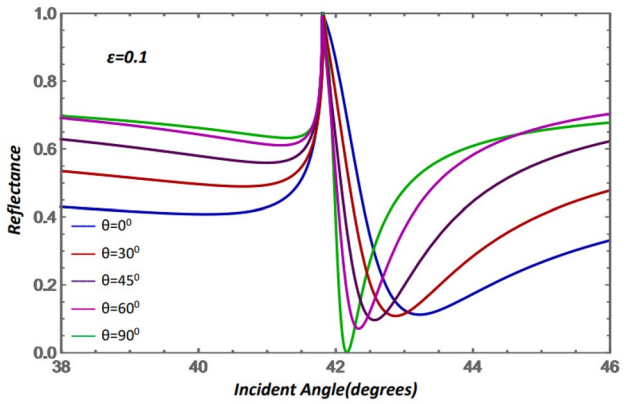

Fig. 3 Dependence of the *p*-polarization reflectance on the incident angle for $\varepsilon_1=2.25$, $\varepsilon_2=1$, frequency of the incident radiation $\omega=6.2832$ *Thz* for different directions of the applied uniaxial strain with $\varepsilon=0.1$, $E_f=0.5$ *eV* and $\varphi=0$

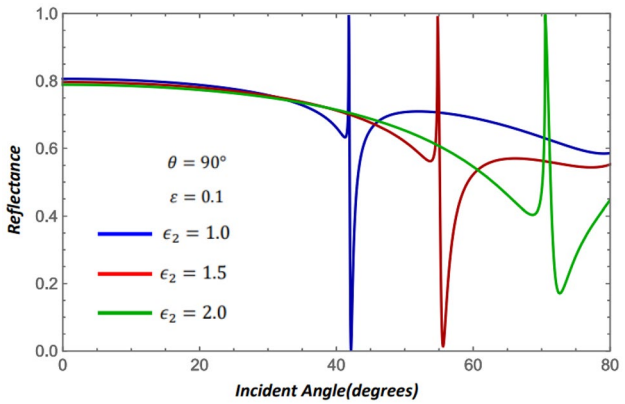

Fig. 5 Dependence of the *p*-polarization reflectance on the incident angle for $\varepsilon_1=2.25$, applied strain $\varepsilon=0.1$, $\theta-\varphi=90°$, $E_f=0.5$ *eV*, $\omega=6.2832$ *Thz*, for different dielectric constant of the sensing medium ε_2

light and surface plasmon is compensated. Once surface plasmon is excited in the Kretschmann configuration, a sharp minimum is observed in the reflection coefficient versus incident angle (or wavelength) curve. Figure 3 shows the variations of the reflectance with the incident angle for different directions of the applied strain and taking the plasmon propagation angle $\varphi=0$. As can be seen, when the angle of the applied strain increases, there is a shift of the resonance peak to lower incident angle and a reduction in the amplitude of the resonance dip. The dip of the surface plasmon resonance curve corresponds to the partial absorption of energy from the incident light to surface plasmons. Thus, it indicates that a greater depth of the dip is better the efficiency of resonance, and this occurs when the applied strain is perpendicular to the direction of the plasmon propagation. In Fig. 4, the reflectance of the monolayer graphene under strain is depicted as a function of the angle of *p*-polarized incident radiation. One important note from this plot is the shift to lower incident angles of the resonance dip in the reflectance when the strain increases for $\theta-\varphi=\pi/2$, i.e., an applied strain perpendicular to the direction of the plasmon propagation. Surface plasmon resonance can be also used to detect biological molecules. This feature is used to design optical biosensors that can measure the refractive index when the biomolecules become adsorbed on the graphene surface and create a layer of refractive index higher than that of the air (ε_2 in Fig. 1), resulting in a change in the resonance angle. Figure 5 plots the theoretical reflectance against the resonance angle for different refractive index of the sensing medium for uniaxial strain with the same magnitude $\varepsilon=0.1$, at $\theta-\varphi=\pi/2$ and for fixed Fermi energy $E_f=0.5$ *eV*. As can be seen, there is a reduction on the amplitude and a shift on the resonance angle of the minimum of the reflectance curve with increasing refractive index of the sensing medium. Therefore, this plasmonic metamaterials

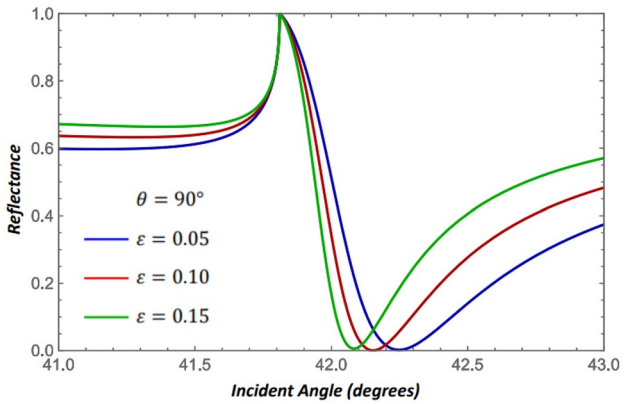

Fig. 4 Dependence of the *p*-polarization reflectance on the incident angle for $\varepsilon_1=2.25$, $\varepsilon_2=1$, frequency of the incident radiation $\omega=6.2832$ *Thz* for different uniaxial strain perpendicular to plasmon propagation, i.e., $\theta-\varphi=90°$ and $E_f=0.5$ *eV*

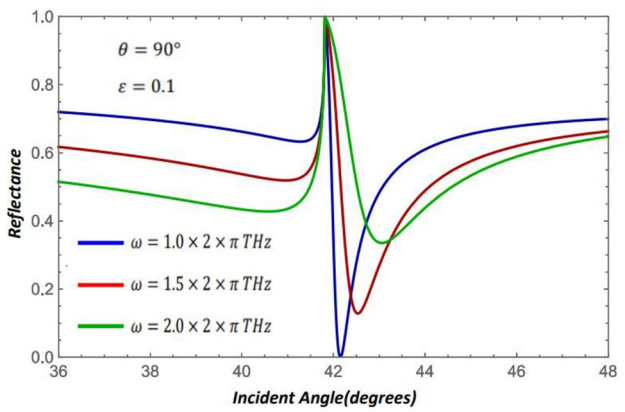

Fig. 6 Shows the dependence of the *p*-polarization reflectance on the incident angle for different frequencies of the incident radiation for $\varepsilon=0.1$, $\theta-\varphi=90°$, $\varepsilon_1=2.25$, $\varepsilon_2=1$ and, $E_f=0.5$ *eV*

are very sensitive to the changes of refractive index of the dielectric media in the vicinity of the graphene layer. On the other hand, Fig. 6 illustrates the reflectance intensity for uniaxial strain with the same magnitude $\varepsilon = 0.1$ for different frequencies of the incident radiation at θ-$\varphi = \pi/2$ and for fixed Fermi energy $E_f = 0.5\ eV$. The reflectance exhibits a maximum dip $\omega = 2\pi THz$ as compared with $\omega = 3\pi THz$ and $\omega = 4\pi THz$, respectively. These important features indicate that the surface plasmon resonances dip with better excitation corresponds to lower frequencies.

Conclusions

In this study, the collective electronic excitations in monolayer graphene structure were investigated under uniaxial strain. Long-range Coulomb interactions in the deformed graphene lead new set of spectra of surface plasmons, which depend on a certain characteristic parameter of the applied strain. These charge density fluctuations can be excited by light using the Kretchmann configuration. Under this configuration, we derived the Fresnel coefficients for oblique incidence of linearly *p*-polarized light through two dielectric media with anisotropic graphene layer at the interface. Based on these generalized coefficients it was demonstrated that the light scattering problem cannot be decoupled in pure *p*-polarized waves. In other words, whenever the nondiagonal conductivity component σ_{xy} is not zero, the incident polarization is not conserved. To illustrate our findings, we consider the uniaxial strain monolayer graphene. The strain effects on the reflectance were estimated as a function either of the magnitude or the strain direction. This opens new possibilities for controlling light-matter interaction on graphene structures.

Author Contribution Corina Lemus made all the mathematical calculations and the numerical analysis in the paper and prepared all the figures. G. González de la Cruz and M Oliva-Leyva wrote the main manuscript text and reviewed the manuscript.

Availability of Data and Materials The authors confirm that the data supporting the findings of this study are available within the article.

Declarations

Ethical Approval Not applicable.

Conflict of Interest The authors declare no competing interests.

References

1. Maier SA (2007) Plasmonics: fundamentals and applications. Springer Science +Busines Media LLC
2. Fei D, Yuanqing Y, Deshpande RA, Bozhevolnyi SI (2018) A review of gap-surface plasmon metasurfaces: fundamentals and applications. Nanophotonics 7:1129
3. Han X, Liu K, Sun C (2019) Plasmonics for biosensing. Materials 12:14111
4. Kravets VG, Jalil R, Kim YJ, Ansell D, Aznakayeva DE, Thackray B, Novoselov KS, Geim A, Grigorenko AN (2014) Graphene-protected copper and silver plasmonics. Sci Rep 4:5517
5. Hailin Xu, Leiming Wu, Dai X, Gao Y, Xiang Y (2016) An ultra-high sensitivity surface plasmon resonance sensor based on graphene-aluminum-graphene sandwich-like structure. J Appl Phys 120:053101
6. Feng Y, Liu Y, Teng J (2018) Design of an ultrasensitive SPR biosensor based on a graphene-MoS2 hybrid structure with a MgF2 prism. Apl Optics 57:3639
7. Patil PO, Pandey GR, Patil AG, Borse VB, Deshmukh PK, Patil DR, Tade RS, Nangare SN, Khan ZG, Patil AM, More MP, Veerapandian M, Bari SB (2019) Graphene-based nanocomposites for sensitivity enhancement of surface plasmon resonance sensor for biological and chemical sensing: a review. Biosens Bioelectron 139:111324
8. Huang S, Song C, Zhang G, Yuan H (2017) Graphene plasmonics: physics and potential applications. Nanophotonics 6:1191
9. Gong W, Jiang S, Li Z, Li C, Xu J, Pan J, Huo Y, Man B, Liu A, Chao C (2019) Experimental and theoretical investigation for surface plasmon resonance biosensor based on graphene/Au film/D-POF. Op Express 27:3483
10. Chen S, Lin C (2019) Figure of merit analysis of graphene-based surface plasmon resonance biosensor for visible and near infrared. Op Commun 435:102
11. Chen S, Lin C (2019) Sensitivity analysis of graphene multilayer based surface plasmon resonance biosensor in the ultraviolet, visible and infrared regions. Appl Phys A 125:230
12. Vahed H, Nadri C (2019) Ultra-sensitive surface plasmon resonance biosensor based on MoS2–graphene hybrid nanostructure with silver metal layer. Opt Quantum Electronics 51:20
13. Sebek M, Elbanna A, Nemati A, Pan J, Shen ZX, Hong M, X., Thanh S.N. and Teng J. (2020) Hybrid plasmonics and two-dimensional materials: theory and applications. J Mol Eng Materials 2:2030001
14. Alam MK, Niu C, Wang Y, Wang W, Li Y, Dai C, Tong T, Shan X, Charlson E, Pei S, Kong XT, Hu Y, Belyanin A, Stein G, Liu Z, Hu J, Wang Z, Bao J (2020) Large graphene-induced shift of surface-plasmon resonances of gold films: effective-medium theory for atomically thin materials. Phys Rev B 2:013008
15. Yari P, Farmani H, Farmani A, Mosavi AM. Monitoring biomaterials with light: review of surface plasmon resonance biosensing using two dimensional materials. https://doi.org/10.20944/preprints202101.0483.v1
16. Kravets VG, Wu F, Yu T, Grigorenko AN (2022) Metal-dielectric-graphene hybrid heterostructures with enhanced surface plasmon resonance sensitivity based on amplitude and phase measurements. Plasmonics 17:973
17. Liu J, Bao S, Wang X (2022) Applications of graphene-based materials in sensors: a review. Micromachines 13:184
18. AlAloul M, Rasras M (2021) Plasmon-enhanced graphene photodetector with CMOS-compatible titanium nitride. J Op Soc Am B 38:602
19. Cui L, Wang J, Mengtao M (2021) Graphene plasmon for optoelectronics. Rev Phys 6:100054
20. Tao L, Chen Z, Li Z, Wang J, Xu X, Xu JB (2021) Enhancing light-matter interaction in 2D materials by optical micro/nano architectures for high-performance optoelectronic devices. InfoMat 3:36
21. Oliva-Leyva M, Naumis G (2013) Understanding electron behavior in strained graphene as a reciprocal space distortion; Phys Rev B 88 085430. Effective Dirac Hamiltonian for anisotropic honeycomb lattices: optical properties. (2016) Phys Rev B 93:035439
22. Men NV, Khanh NQ, Phuong DTK (2019) Plasmon modes in MLG-2DEG heterostructures: temperature effects. Phys Lett A 383:1364
23. Men NV, Khanh NQ, Phoung DTK (2021) Collective excitations in spin-polarized bilayer graphene. J Phys Condens Matter 33:105301

24. Men NV, Phoung DTK (2021) Temperature effects on plasmon modes in double-bilayer graphene structures. Solid State Commun 334:114398
25. Men NV (2022) Temperature and inhomogeneity combination effects on collective excitations in three-layer graphene structures. Physica E 140:115201
26. Men NV, Khanh NQ, Linh DK (2022) Plasmon modes in double-layer biased bilayer graphene. Physica B 625:413501
27. Naumis GG, Barraza-Lopez S, Oliva-Leyva M, Terrones H (2017) Electronic and optical properties of strained graphene and other strained 2D materials: a review. Rep Prog Phys 80:096501
28. Ma Z, Cai W, Xiang Y, Ren M, Zhang X, Jingjun Xu (2017) Dynamic spontaneous emission control of an optical emitter coupled to plasmons in strained graphene. Op Express 25:23070
29. Roldán R, Castellanos-Gomez A, Cappelluti E, Guinea F (2015) Strain engineering in semiconducting two-dimensional crystals. J Phys Condens Matter 27:313201
30. Kuang Y, Lindsay L, Shi S, Wang X, Hang B (2016) Thermal conductivity of graphene mediated by strain and size. Int J Heat Mass Transfer 101:772
31. Pellegrino FMD, Angilella GGN, Pucci R (2012) Effect of uniaxial strain on plasmon excitations in graphene. J Phys Conf Ser 377:012083
32. Dahal D, Gumbs G, Huang D (2018) Effect of strain on plasmons, screening, and energy loss in graphene/substrate contacts. Phys Rev B 98:045427
33. Oliva-Leyva M, Gonzalez de la Cruz G (2019) Unveiling optical in-plane anisotropy of 2D materials from oblique incidence of light. J Phys Condens Matter 31:33570
34. Hayn R, Wei T, Silkin VM, Van den Brink J (2021) Plasmons in anisotropic Dirac systems. Phys Rev Matter B 106:075103
35. Poya S, Vazifehshenas T, Saleh M, Farmanbar M, Salavati-Fard T (2018) Plasmon modes in monolayer and double-layer black phosphorus under applied uniaxial strain. J Appl Phys 123:174301
36. Peng Z, Chen X, Fan Y, Srolovitz DJ, Lei D (2020) Strain engineering of 2D semiconductors and graphene: from strain fields to band-structure tuning and photonic applications. Light Sci Appl 9:190
37. Oliva-Leyva M, Naumis G (2016) Effective Dirac Hamiltonian for anisotropic honeycomb lattices: optical properties. Phys Rev B 93:035439
38. Kubo R, Toda M, Hashitsume N (1991) Statistical Physiscs II. Springer Verlag, Nonequilibrium Statistical mechanics
39. Hwang EH, Das SS (2007) Dielectric function, screening, and plasmons in two-dimensional graphene. Phys Rev B 75:205418
40. Usik MO, Bychkov IV, Shavrov VG, Kuzmin DA (2019) Surface plasmon-polaritons in deformed graphene excited by attenuated total internal reflection. Open Mater Sci 5:7
41. Ardakania AG, Ghasemi Z, Golshan MM (2017) A new transfer matrix for investigation of surface plasmon modes in multilayer structures containing anisotropic graphene layers. Eur Phys J Plus 132:206
42. Zhan T, Shi X, Dai Y, Liu X, Zi J (2013) Transfer matrix method for optics in graphene layers. J Phys Condens Matter 25:215301